A Probabilistic Method for the Detection of Obstructed Cracks of Beam-type Structures Using Spatial Wavelet Transform

H.F. Lam* and C.T. Ng

Department of Building and Construction, City University of Hong Kong, 83 Tat Chee Avenue, Kowloon, Hong Kong

* Corresponding author:

Tel.: +852 2788-7303

Fax: +852 2788-7612

Email: paullam@cityu.edu.hk

Keywords: Multiple crack detection; Bayesian model class selection; Bayesian statistical framework; Spatial wavelet transform.

A Probabilistic Method for the Detection of Obstructed Cracks of Beam-type Structures Using Spatial Wavelet Transform

H. F. Lam and C. T. Ng

Department of Building and Construction, City University of Hong Kong, Hong Kong Special Administrative Region, China

Abstract:

This paper reports both the theoretical development and the numerical verification of a practical wavelet-based crack detection method, which identifies first the number of cracks and then the corresponding crack locations and extents. The value of the proposed method lies in its ability to detect obstructed cracks when measurement at or close to the cracked region is not possible. In such situations, most non-model based methods, which rely on the abnormal change of certain indicators (e.g., curvature and strain mode shapes) at or close to the cracks, cannot be used. Most model-based methods follow the model updating approach. That is, they treat the crack location and extent as model parameters and identify them by minimizing the discrepancy between the modelled and measured dynamic responses. Most model-based methods in the literature can only be used in single- or multi-crack cases with a given number of cracks. One of the objectives of this paper is to develop a model-based crack detection method that is applicable in a general situation when the number of cracks is not known in advance.

To explicitly handle the uncertainties associated with measurement noise and modelling error, the proposed method uses the Bayesian probabilistic approach. In particular, the method aims to calculate the posterior (updated) probability density function (PDF) of the crack locations and the corresponding extents.

The proposed wavelet-based crack detection method is verified and demonstrated through a comprehensive series of numerical case studies, in which noisy data were generated by a Bernoulli-Euler beam with semi-rigid connections. The results show that the method can correctly identify the number of cracks even when the crack extent is small. The effects of the number of cracks and the crack extents on the results of crack detection are also studied and discussed in this paper.

1 Introduction

In recent years, developments in sensor technologies, data storage devices and high-speed computing have been so fast that the use of measured vibration data in structural damage detection (or health monitoring) has become feasible from a hardware point of view. However, the development of software tools for the reliable detection and characterisation of structural damage is still lacking, which prevents the exploitation of the full potential of the technique. In-situ structural health monitoring is part of a current revolution in smart-structure technologies that promises quantum gains in performance, endurance and cost-efficient maintenance for high-value assets in civil, mechanical and aerospace engineering. Many methods have been developed for detecting various types of damage (e.g., cracks on beams, reduction in the stiffness of structural members and connections, and degradation of materials) to various types of structures (e.g., trusses, frames, buildings and bridges) under different assumptions (e.g., linear elastic, time-invariant) and making use of different measured quantities (e.g., time-domain responses, modal parameters and wavelet transform). A comprehensive review of SHM methods from 1996 to 2001 was conducted by Sohn et al. (2004).

Wavelet analysis has been one of the fastest evolving signal processing tools in the area of damage detection (Sohn et al. 2004). In 2000, Hou et al. (2000) proposed a wavelet-based approach to structural damage detection, and verified the approach by simulated data of a simple structural model with multiple breakable springs under harmonic excitation. In the same year, Okafor and Dutta (2000) used both computer simulated and experimental measured data to prove the usefulness of wavelet transform in structural damage detection. Very encouraging results were obtained. Two years later, Yan and Yam (2002) presented a wavelet-based method for the detection of cracks within a small area on a composite plate using embedded piezoelectric patches as actuator and sensors. Sun and Chang (2003) proposed the use of wavelet packet transform to detect structural damage with the help of neural networks. All of the abovementioned methods carried out the wavelet transform in the time-domain. In contrast, Liew and Wang (1998) proposed for the first time to undertake the wavelet transform in the space-domain, which was found to be very sensitive to structural cracks. In 1999, Wang and Deng (1999) extended the approach to develop a wavelet-based method for crack detection in beam and plate structures. Lu and Hsu (2002) presented a defect detection method for uniform string by comparing the spatial wavelet transform before and after damage. Chang and Chen (2003) proposed the use of spatial wavelet transform in the detection of a crack on a Timoshenko beam, which was modelled as a rotational spring, and numerically verified their method. Lam et al. (2005) carried out a feasibility study on the use of the Bayesian approach to calculate the posterior (updated) probability density function (PDF) of crack parameters,

such as crack location and extent. The method not only identifies the crack location and extent, but also the corresponding uncertainties. The results of the numerical case studies are very encouraging. Spanos et al. (2006) proposed a damage detection method in a Bernoulli-Euler beam subjected to static loads via spatial wavelet transform.

The main purpose of this paper is to extend the idea of Lam et al. (2005) to form a practical crack detection method that is suitable for multiple cracks even when they are obstructed. Most existing non-model based methods rely on the changes in measured quantity (e.g., displacement mode shape and strain mode shape) at the crack or in the close neighbourhood of the cracked region. However, if measurements at or near the cracks are obtainable, the inspector should have no problem in directly observing the crack or damage. The value of a crack detection method will be much higher if it can detect cracks even when it is not possible to take measurement in the neighbourhood of the cracked region. The numerical case studies presented in this paper clearly show that the proposed crack detection method is applicable even when the measurement of the reference (healthy) structure and the system input (excitation) are not available. By following the probabilistic approach, the uncertainties associated with the uncertain system parameters, such as the damping ratio and the semi-rigid behaviour of the beam end connections, can be explicitly handled.

The remainder of this paper is organised as follows. The proposed method is presented in section 2, and the related background theories, such as the modelling of beams with multiple cracks, the wavelet transform and the Bayesian approach, are reviewed. Section 3 reports the results of a series of comprehensive numerical case studies, which verify and demonstrate the proposed method. These case studies produced very encouraging results. The effects of crack number and crack extent in the results of crack detection are discussed based on the results of these case studies. Conclusions are drawn at the end of the paper.

2 Proposed Methodology and Background Theories

2.1 Modelling and parameterisation of beams with multiple cracks

The free vibration of a Bernoulli-Euler beam of length L is governed by:

$$EI\frac{\partial^4 y(x,t)}{\partial x^4}+m\frac{\partial^2 y(x,t)}{\partial t^2}=0 \tag{1}$$

where EI is the flexure rigidity, m is the mass density (mass per unit length) and y is the transverse deflection of the beam. By the separation of variables, we have $y(x,t)=\phi(x)z(t)$, where $z(t)$ is the modal amplitude and $\phi(x)$ is the mode shape function governed by:

$$\frac{d^4\phi(x)}{dx^4} - \beta^4\phi(x) = 0 \tag{2}$$

where $\beta^4 = \omega^4 m / EI$, and ω is the angular natural frequency of the system in radians per second. Figure 1 shows the model of a beam with N_C cracks. The beam is divided into $N_C + 1$ segments, each with length l_i, for i = 1, …, $N_C + 1$, where $\sum_{i=1}^{N_C+1} l_i = L$. The solution of the ϕ function for each segment can be calculated by considering the boundary and continuity conditions. The four boundary conditions are:

$$\begin{aligned}
&\phi_1(0) = \phi_{N_C+1}\left(l_{N_C+1}\right) = 0 \\
&K_L \frac{d\phi_1(0)}{dx} = EI \frac{d^2\phi_1(0)}{dx^2} \\
&K_R \frac{d\phi_{N_C+1}\left(l_{N_C+1}\right)}{dx} = -EI \frac{d^2\phi_{N_C+1}\left(l_{N_C+1}\right)}{dx^2}
\end{aligned} \tag{3}$$

where K_L and K_R are the stiffness coefficients of the rotational springs at the left and right ends of the beam respectively. The rotational springs model the semi-rigid behaviour of the beam end connections (Chen and Kishi 1989). At the general *i*th segment of the beam, the following four continuity conditions must be satisfied:

$$\begin{aligned}
&\phi_i(l_i) = \phi_{i+1}(0) \\
&\frac{d\phi_{i+1}(0)}{dx} - \frac{d\phi_i(l_i)}{dx} = \Delta_i L \frac{d^2\phi_{i+1}(0)}{dx^2} \\
&\frac{d^2\phi_i(l_i)}{dx^2} = \frac{d^2\phi_{i+1}(0)}{dx^2} \\
&\frac{d^3\phi_i(l_i)}{dx^3} = \frac{d^3\phi_{i+1}(0)}{dx^3}
\end{aligned} \tag{4}$$

where $i = 1, ..., N_C$; Δ_i is the non-dimensional flexibility parameter that characterises the extent of the *i*th crack. The relationship between the crack extent Δ_i and the crack depth ratio $\delta_i = a_i / h$ can be found in Ostachowicz et al. (1991). The detailed formulation is not presented in this paper due to the limited space.

A characteristic equation can be obtained by considering the boundary and continuity conditions. An infinite number of solutions can then be calculated and denoted by β_k for $k = 1, \ldots . \infty$. For each β_k, the natural frequencies ω_k and mode shape ϕ_k of the system can be computed, and the overall response of the beam can be calculated by modal superposition.

According to Katafygiotis et al. (2000), the uncertainties associated with the stiffness of the rotational spring (K_L and K_R in equation (3)) are much larger than those associated with other model parameters, such as the modulus of elasticity and the mass density of the structural member. Therefore, the rotational stiffnesses are included as uncertain parameters in the proposed crack detection method. For a given set of measurements, an increase in the uncertainties associated with the crack detection results is the trade-off for including additional uncertain parameters (Lam and Ng 2006). The numerical values of the rotational stiffnesses are of a different order of magnitude to other uncertain parameters. To prevent a numerical problem, the rotational stiffnesses are normalized by the bending rigidity of the beam:

$$\tilde{K}_L = \frac{K_L}{EI} \quad \text{and} \quad \tilde{K}_R = \frac{K_R}{EI} \tag{5}$$

where $\tilde{K}_L$ and $\tilde{K}_R$ are the normalized rotational stiffnesses at the left and right ends of the beam respectively.

The reference system (healthy status) is represented by the model class M_0 ($j = 0$), in which the vector of uncertain model parameters is $\mathbf{a}_0 = \{\tilde{K}_L, \tilde{K}_R, \zeta\}^T$, where the subscript of $\mathbf{a}$ represents the number of cracks. Because the bending rigidity (EI) and the mass density (ρ) can usually be measured or calculated with a high degree of accuracy, they are not included as uncertain parameters in the numerical case study. In general, the uncertain parameter vector for the class of models with j cracks, M_j, is:

$$\mathbf{a}_j = \left\{\tilde{K}_L, \tilde{K}_R, \zeta, l_1, l_2, \mathrm{K}\ l_j, \Delta_1, \Delta_2, \mathrm{K}\ , \Delta_j\right\}^T \tag{6}$$

The total number of uncertain parameters is $2j+3$. It is assumed that the damping ratios for all modes are the same and equal to ζ to reduce the number of uncertain parameters.

2.2 Spatial wavelet transform and its application to crack detection

To ensure that this paper is self-contained, the spatial wavelet transform of the deflection curve of a beam is briefly reviewed in this section. Interested readers are directed to Liew and Wang (1998) for more detail. Both the real and imaginary parts of the spatial wavelet transform of the deflection curve are very sensitive to cracks. A deflection curve $y(x,t)$, which can be obtained by experimental measurement or computer simulation, can be decomposed into harmonic functions defined in $0 \le x \le L$ by using the following two sets of wavelet expressions:

$$W_1(x)=\sin\left(2\pi\frac{x}{L}\right) \quad \text{and} \quad W_2(x)=\cos\left(2\pi\frac{x}{L}\right) \tag{7.}$$

The beam displacement at a particular point, x, and time, t, can be represented in terms of a constant. a_0, plus the contributions from all of the wavelets (Liew and Wang 1998; Lee and Liew 2001). Therefore,

$$y(x,t)=a_0+\sum_{k=0}^{\infty}\sum_{b=0}^{2^k-1}a_{2^k+b}W\left(2^k x-b\right) \tag{8.}$$

where b is the translation parameter indicating the position, 2^k is the scale parameter, $W(x)=W_1(x)+iW_2(x)$, and $a_{2^k+b}=\Re\left(a_{2^k+b}\right)+i\Im\left(a_{2^k+b}\right)$ is a complex number. The real $\Re\left(a_{2^k+b}\right)$ and imaginary $\Im\left(a_{2^k+b}\right)$ parts of a_{2^k+b} can be expressed as:

$$\Re\left(a_{2^k+b}\right)=2^k\int_0^L y(x,t)W_2\left(2^k x-b\right)dx \quad \text{and} \quad \Im\left(a_{2^k+b}\right)=2^k\int_0^L y(x,t)W_1\left(2^k x-b\right)dx \tag{9.}$$

To explain the basic idea of the proposed crack detection method, an example of a simply supported beam with unit length (L = 1 m) and two cracks at 0.55 m and 0.64 m from the left end of the beam is considered. Figure 2 shows the real and imaginary parts of the spatial wavelet transformation of the deflection curve. Considering the real part in Figure 2, the two cracks are indicated by two "impulse" type discontinuities in the graph. After the discontinuity, the curve goes back to a value that is very close to the original value before the discontinuity. Although the "impulses" are very sharp, the effect is very local and affects only the very close neighbours of the cracks. In the imaginary part, the cracks are indicated by two "jump" type discontinuities. Unlike the discontinuities in the real part, the curve will not restore the original value after the discontinuities. As a result, the effect of cracks in the imaginary part is not as local as that in the real part. When measurement is available throughout the entire beam, both the real and imaginary parts provide valuable information for detecting the cracks. However, the situation is very different if the cracks are obstructed and measurement at the region close to the cracks is not available.

Figure 3 shows the same graph as Figure 2 except the region near the cracks is obstructed. Let us first consider the real part in Figure 3. When the two ends of the curve immediately outside the obstruction are extended, the two extended curves are very consistent and even concurrent. As a result, it is not possible to tell if there is any crack in the obstructed region by looking at the real part alone. When the imaginary part is considered, the two extended curves are very far away from each other, thus showing that there must be one or more "jumps" in the obstructed region. This

simple illustrative example shows that the imaginary part of the spatial wavelet transformation of the deflection curve contains information on the cracks even when the cracks are obstructed.

2.3 Identification of the number of cracks by the Bayesian model class selection method

In general, the model-based crack detection method adopts different classes of models for beams with different numbers of cracks. In Figure 4, the model class M_j is employed in modelling a beam with *j* cracks for $j = 0,\ldots,N_M$, where N_M is the maximum number of cracks to be considered and the parameters l_j and Δ_j are used to describe the location and extent of the *j*th crack. Using this formulation, the identification of the number of cracks is equivalent to selecting the "best" model class. It must be pointed out that the selection of the "best" model class based on a given set of data *D* is not trivial. It is clear that the model class of a beam with more cracks consists of more model parameters (e.g., M_2 has two more model parameters, l_2 and Δ_2, than M_1, as shown in Figure 4). A model class with more parameters can provide a better fit to the measurement when compared to a model class with fewer parameters. Therefore, the selection of model class based solely on the fitting between the modelled and the measured dynamic responses can be very misleading, as the most complex model class will always be selected.

A computationally efficient algorithm is developed for the identification of the number of cracks utilizing the set of measured wavelet transformation. The proposed algorithm involves the calculation of the conditional probability $P(M_j \mid D,U)$, which is the probability of a model class M_j for a given set of data *D* and engineering judgement *U*. The procedures of the proposed algorithm are as follows.

1. Initialize the index $j = 0$, and calculate the conditional probability $P(M_j \mid D,U) = P\left(M_0 \mid D,U\right)$ for the beam without a crack.
2. Increase the index *j* by 1 ($j = j + 1$), and calculate the conditional probability $P(M_j \mid D,U) = P\left(M_1 \mid D,U\right)$ for the beam with a single crack.
3. Compare the values of the conditional probabilities $P(M_{j-1} \mid D,U)$ and $P(M_j \mid D,U)$. If $P(M_{j-1} \mid D,U) > P(M_j \mid D,U)$, then M_{j-1} is the "best" model class. Otherwise, increase the index *j* by 1 ($j = j + 1$) and repeat this step.

The question now is the way to calculate the conditional probability $P(M_j \mid D,U)$. The goal here is to use the set of measured dynamic data D to select the "best" class of models from amongst N_M+1 prescribed classes of models. $\mathbf{a}_j \in S(\mathbf{a}_j) \subset R^{N_j}$ is the vector of uncertain parameters, which is defined in equation (6), to be identified following the Bayesian statistical framework, where N_j is the dimension of $\mathbf{a}_j$. By following the Bayes' theorem, the conditional probability can be formulated as (Beck and Yuen 2004):

$$P(M_j \mid D,U) = \frac{p(D \mid M_j,U)P(M_j \mid U)}{p(D \mid U)} \quad \text{for} \quad j = 0,...,N_M \tag{10}$$

where $p(D \mid U) = \sum_{j=0}^{N_M} p(D \mid M_j,U)p(M_j \mid U)$ by the theorem of total probability, and $1/p(D \mid U)$ can be treated as a normalizing constant. $P(M_j \mid U)$ is the prior probability of model class M_j based on engineering judgment, where $\sum_{j=0}^{N_M} P(M_j \mid U) = 1$. Unless there is prior information about the number of cracks on the beam, the prior probability $P(M_j \mid U)$ can be taken as $1/(N_M+1)$. The most important term in equation (10) is the evidence $p(D \mid M_j,U)$ for the model class M_j provided by the data D. It must be pointed out that U is irrelevant in $p(D \mid M_j,U)$ because it is assumed that M_j alone specifies the PDF for the data. Therefore, we have $p(D \mid M_j) = p(D \mid M_j,U)$.

For a globally identifiable case, the evidence can be calculated based on an asymptotic approximation (Papadimitriou et al. 1997):

$$p(D \mid M_j) \approx p(D \mid \hat{\mathbf{a}}_j, M_j)(2\pi)^{\frac{N_j}{2}} p(\hat{\mathbf{a}}_j \mid M_j)\left|\mathbf{H}_j(\hat{\mathbf{a}}_j)\right|^{-\frac{1}{2}} \quad \text{for} \quad j = 0,\ldots,N_M \tag{11}$$

where $\hat{\mathbf{a}}_j$ denotes the optimal model in the model class M_j (the set of optimal model parameters $\mathbf{a}_j$). $\hat{\mathbf{a}}_j$ can be obtained by maximizing the posterior PDF $p(\mathbf{a}_j \mid D,M_j)$, N_j is the number of uncertain model parameters in $\hat{\mathbf{a}}_j$, and $\mathbf{H}_j(\hat{\mathbf{a}}_j)$ is the Hessian of the function $g(\mathbf{a}_j)$ evaluated at the optimal model $\hat{\mathbf{a}}_j$, where $g(\mathbf{a}_j)$ is given by:

$$g(\mathbf{a}_j) = -\ln[p(\mathbf{a}_j \mid M_j)p(D \mid \mathbf{a}_j, M_j)] \tag{12}$$

For unidentifiable cases, the evidence $p(D \mid M_j)$ can be calculated by using an extension of the asymptotic expansion used in equation (11) (Beck and Katafygiotis 1998; Katafygiotis et al. 1998). The discussion here will focus on globally identifiable cases. Interested readers are directed to

Katafygiotis et al. (1998, 2000) and Katafygiotis and Lam (2002) for details of the classification of identifiable and unidentifiable problems and the approximation of the likelihood $p(D \mid \mathbf{a}_j, M_j)$ in the general unidentifiable problem.

The evidence $p(D \mid M_j)$ in equation (11) consists of two factors. The first factor $p(D \mid \hat{\mathbf{a}}_j, M_j)$ is the likelihood factor. This will be larger for those model classes that make the probability of the data D higher, that is, those that give a better "fit" to the data, which favours model classes with more parameters. The second factor $(2\pi)^{N_j/2}\ p(\hat{\mathbf{a}}_j \mid M_j) \mid \mathbf{H}_j(\hat{\mathbf{a}}_j) \mid^{-1/2}$ is called the Ockham factor (Gull 1988). Beck and Yuen (2004) showed that the value of the Ockham factor decreases as the number of uncertain parameters in the model class increases, and it therefore provides a mathematically rigorous and robust penalty against parameterization.

The proposed computationally efficient algorithm can identify the number of cracks, say N_C, by calculating the conditional probability $P(M_j \mid D,U)$ of the model classes M_0, M_1, …, M_{N_C+1}. The maximum number of cracks to be considered N_M is equal to N_C+1.

2.4 Detection of crack locations and extents by the Bayesian statistical framework

After identifying the number of cracks, for example N_C, the goal is to calculate the posterior PDF $p(\mathbf{a}_{N_C} \mid D, M_{N_C})$ of the set of uncertain parameters $\mathbf{a}_{N_C}$ in the model class M_{N_C} by following the Bayesian statistical framework. Due to the limited space, only the most important equations are given in this paper. Interested readers are referred to Lam et al. (2005) for the detailed procedures.

The posterior PDF of the model parameters $\mathbf{a}_{N_C}$ for the given set of dynamic measurement D and model class M_{N_C} can then be approximated as a weighted sum of Gaussian distributions centred at the N_q optimal models:

$$p(\mathbf{a}_{N_C} \mid D, M_{N_C}) \approx \sum_{q=1}^{N_q} w_q \mathbf{N}\left(\hat{\mathbf{a}}_{N_C}^{(q)}, A_N^{-1}\left(\hat{\mathbf{a}}_{N_C}^{(q)}\right)\right) \tag{13}$$

where $\mathbf{N}(\boldsymbol{\mu}, \boldsymbol{\Sigma})$ denotes a multivariate Gaussian distribution with mean $\boldsymbol{\mu}$ and covariance matrix $\boldsymbol{\Sigma}$. The covariance matrix $A_N^{-1}\left(\hat{\mathbf{a}}_{N_C}^{(q)}\right)$ is the Hessian of the function $N_J \ln J(\mathbf{a}_{N_C} \mid D, M_{N_C})$ evaluated at $\hat{\mathbf{a}}_{N_C}^{(q)}$, where $J(\mathbf{a}_{N_C} \mid D, M_{N_C})$ is given by:

$$J\left(\mathbf{a}_{N_C} \mid D, M_{N_C}\right) = \frac{1}{NN_N}\sum_{n=1}^{N}\left\|\Im\left[\mathbf{p}(n)\right] - \Im\left[\mathbf{q}\left(n;\mathbf{a}_{N_C}\right)\right]\right\|^2 \tag{14}$$

where N_N is the number of observed locations, $\mathbf{p}(n)$ is the measured deflection curve at the nth time step, $\Im[\mathbf{x}]$ is the imaginary part of the wavelet transformation of the $\mathbf{x}$ vector and $\mathbf{q}\left(n;\mathbf{a}_{N_C}\right)$ is the calculated deflection curve of the model $\mathbf{a}_{N_C}$ at the nth time step. The weighting coefficients in equation (13) are given by:

$$w_q = \frac{w_q'}{\sum_{q=1}^{N_q} w_q'} \text{ where } w_q' = \pi\left(\hat{\mathbf{a}}_{N_C}^{(q)}\right)\left|A_N\left(\hat{\mathbf{a}}_{N_C}^{(q)}\right)\right|^{-\frac{1}{2}} \tag{15}$$

where $\pi\left(\hat{\mathbf{a}}_{N_C}^{(q)}\right)$ is the prior PDF $p\left(\mathbf{a}_{N_C} \mid M_{N_C}\right)$ of the set of uncertain model parameters $\mathbf{a}_{N_C}$ evaluated at $\hat{\mathbf{a}}_{N_C}^{(q)}$. Instead of pinpointing the crack locations and extents, the proposed crack detection method focuses on calculating the posterior PDF of the parameters $\mathbf{a}_{N_C}$. As a result, the level of confidence in the results of crack detection can be quantified. This information is extremely important for engineers who are making judgments about remedial work.

3 Numerical Verification

A Bernoulli-Euler beam is employed as a verification example, and the sectional and material properties of the beam are summarized in Table 1. The system is assumed to be classically damped with a damping ratio of 0.01 (1%) for all modes. The two supports of the beam are neither pin nor rigid but semi-rigid, and are modelled by rotational springs. In all cases, the beam is vibrated by an impact hammer at 0.4m from the left end of the beam. It is assumed that optical equipment is employed to measure the time-domain displacement responses of the beam at the unobstructed region. As this equipment is able to provide precise measurements, only 3% white noise is added to the calculated responses for simulating measurement noise. The measured time duration is 0.4sec with 0.01sec time step. It is assumed that the beam is obstructed from 0.5m to 0.75m, and the measured responses within this range are not available.

In this paper, six cases (Cases A to F) are considered to verify and demonstrate the proposed crack detection method. The simulated crack locations and crack extents together with the rotational spring stiffness at the two end connections of all cases are summarized in Table 2. Case A considers an undamaged situation. In Case B, there is only one crack at l_1 = 0.55m with crack extent Δ_1 = 0.03 (corresponding to a crack depth of 49% of the beam depth). There is also only one crack in Case C but the crack extent Δ_1 = 0.01 (30% of the beam depth) is smaller than that in Case B. This

case is dedicated to test the performance of the proposed method when the crack is small. Cases D and E have two cracks, which are located at 0.55m and 0.64m from the left end of the beam, respectively. The crack extents are $\Delta_1 = 0.03$ and $\Delta_2 = 0.05$ in Case D and both crack extents are equal to 0.01 in Case E. Again, Case E can test the effect of small cracks in the proposed method. Finally, Case F is used to test the proposed method when there are three cracks. The cracks are located at $l_1 = 0.55$m, $l_2 = 0.09$m and $l_3 = 0.06$m, and the corresponding extents are $\Delta_1 = 0.03$, $\Delta_2 = 0.05$ and $\Delta_3 = 0.04$.

4 Results and Discussion

4.1 Identification of the number of cracks

Table 3 shows the results of the proposed algorithm in identifying the number of cracks in all cases. As the numerical values of the evidence, the likelihood factor and the Ockham factor are very large, which can cause computational problems, only their logarithmic values are calculated and presented. The most important information in Table 3 is the relative probability of the model class M_j for given data D and engineering judgement U. For ease of comparison, the relative probability is normalized such that the largest one is equal to unity. The number of cracks can be identified by selecting the model class with the highest relative probability in Table 3. It is clear from the table that model class M_0 is selected in Case A. In Cases B and C, model class M_1 is selected. Model class M_2 is selected in Cases D and E, while model class M_3 is selected in Case F. It is very clear that the proposed crack detection method successfully identifies the number of cracks in all cases.

As shown in the formulation, the higher the value of the likelihood factor, the better the fit between the measured and modelled responses will be. Table 3 clearly shows that the logarithm of the likelihood factor is always larger for model classes with higher complexity (more cracks). Therefore, it is impossible to use the likelihood factor alone in selecting the "best" model class to identify the number of cracks. The Ockham factor is an important factor for penalizing the parameterization of a model class. It is also clear from Table 3 that the value of the Ockham factor decreases (i.e., its logarithm becomes more negative) for more complex model classes.

4.2 Identification of crack parameters

After identifying the number of cracks, the proposed method can be used to calculate the posterior PDF of both the crack parameters (i.e., crack locations and extents) and the model parameters (e.g., the rotational stiffness). In this section, the identified crack parameters are discussed first.

Table 4 summarises the results of the identified crack locations and extents for all cases. The coefficients of variation (COV) of the identified crack parameters are calculated based on the updated PDFs. They are presented inside the brackets in Table 4. As there is no crack in Case A, the identified crack location and extent for this case are not available.

In Case B the identified crack location and extent are l_1 = 0.5499 m and Δ_1 = 0.0307, respectively. These results are very close to the true values of 0.55 m and 0.03, respectively, as shown in Table 2. The normalized marginal PDF of the crack location and extent (l_1 and Δ_1) in Case B is plotted in Figure 5. It is clear from the figure that there is only one peak, and that the PDF value drops rapidly when one moves away from the peak in any direction. This is a typical characteristic of an identifiable case (Katafygiotis and Lam 2002). The marginal cumulative distributions of all crack parameters can then be obtained and plotted in Figures 6 and 7. These figures provide detailed information on the uncertainties associated with the identified crack parameters. It is very clear that the uncertainty associated with the identified crack location is smaller than that associated with the identified crack extent. This argument can be reinforced by referring to the corresponding COV values given in Table 4. The COV values of the identified crack location and extent are 0.12 and 1.74, respectively.

The crack location in Case C is the same as that in Case B, but the crack extent is reduced to Δ_1 = 0.01. As show in Table 4, the identified crack location and extent for Case C are l_1 = 0.5502 m and Δ_1 = 0.0064, respectively. These identified values are very close to the true values (l_1 = 0.55 m and Δ_1 = 0.01) as shown in Table 2. The normalized marginal PDF of crack parameters is plotted in Figure 8. When this figure is compared to Figure 5, the drop in PDF value away from the peak for Case B (Figure 5) is much faster than that for Case C (Figure 8). This implies that the uncertainties of the identified crack parameters in Case C are higher than those in Case B.

To clearly show this effect in an individual crack parameter, the marginal cumulative distribution of the crack location (l_1) and extent (Δ_1) of Case C are plotted in Figures 9 and 10, respectively. Comparing Figures 6 and 9, it can be concluded that the identified crack location in Case B is less uncertain than that in Case C. Furthermore, it is very clear that the uncertainty of the identified crack extent for Case C is much higher than that for Case B by comparing Figures 7 and 10. This result is expected, as the crack extent in Case C is much smaller than that in Case B, which means that the crack is more outstanding in Case B. This argument is further reinforced by referring to the COV values of the identified crack location (0.34) and crack extent (3.93) in Case C of Table 4.

Cases D and E are used to verify the proposed crack detection method when there are two cracks in the obstructed region. In particular, Case E is considered to test the proposed method

when the cracks are small. By comparing the identified and simulated crack parameters, it can be concluded that the results of crack detection are good but not as accurate as cases with only one crack (i.e. Cases B and C). For example, the identified crack locations in Case D are l_1 = 0.5403m and l_2 = 0.0945m, while the simulated crack locations are l_1 = 0.55m and l_2 = 0.09m. It can be observed from Table 4 that the COV values in Case D (large crack extents) are smaller than those in Case E (small crack extents). This result is consistent with that from the comparison between Cases B and C – the smaller the crack extent, the higher will be the uncertainty associated with the identified results.

In Case F, the identified crack locations are l_1 = 0.5513m, l_2 = 0.0873m and l_3 = 0.0586m, and the identified crack extents are Δ_1 = 0.0326, Δ_2 = 0.0465 and Δ_3 = 0.0436. The identified crack parameters are close to the simulated parameters as shown in Table 2. This series of case studies clearly demonstrates the ability and performance of the proposed wavelet-based crack detection method in detecting multiple cracks even when those cracks are hided.

4.3 Identification of model parameters

To consider the semi-rigid behaviour at the beam end connections, the two supports of the beam are modelled by two rotational springs with different rotational stiffnesses. There is no simple way to measure or calculate the exact value of this type of rotational stiffness. In the proposed method, these two rotational spring constants together with the damping ratio are treated as uncertain model parameters to be identified together with the crack parameters. Table 5 summarizes the optimal model parameters and the corresponding COV values.

In all cases, the identified normalized rotational spring stiffness of the left and right end connections vary from 0.38 to 0.42 and from 0.14 to 0.22, respectively. They are all very close to the simulated values ($K_L^{\%}$= 0.4 and $K_R^{\%}$= 0.2) that are shown in Table 2. When comparing the COV values of the identified rotational stiffnesses in Table 5 to the COV values of the crack parameters in Table 4, the uncertainties associated with the identified rotational stiffnesses are generally higher than those associated with the identified crack parameters. The identified damping ratios in all cases are very close to the simulated values that are shown in Table 2.

5 Concluding Remarks

This paper addresses the problem of crack detection in beams by using the spatial wavelet transformation of the deflection curve following the probabilistic approach. Unlike other crack

detection methods from the literature, the proposed method is applicable in multi-crack cases even when the cracks are obstructed and measurement at or near the cracks is not available. The proposed method relies on the imaginary part of the spatial wavelet transformation in providing useful information for crack detection. Furthermore, the proposed method adopts the Bayesian approach in extracting useful information from the measurement for identifying (1) the number of cracks, (2) the crack locations and extents and (3) the uncertain model parameters, such as the rotational stiffness at the two ends of the beam. By following the Bayesian approach, the proposed method calculates the updated PDF of the crack and model parameters. As a result, the uncertainties associated with the crack detection results can be explicitly handled.

A Bernoulli-Euler beam with semi-rigid connections at both ends is employed to verify the proposed method in a series of numerical case studies. The results are very encouraging because the proposed method can detect the simulated cracks in all cases in the presence of measurement noise. According to the case study results, it can be concluded that the uncertainties associated with crack detection results depend on the number of cracks and the corresponding crack extents. Generally, those uncertainties are higher for cases with more cracks and for cases with cracks of smaller extents.

6 Acknowledgement

The work described in this paper was fully supported by a grant from the Research Grants Council of the Hong Kong Special Administrative Region, China (Project No. CityU 1190/04E).

7 References

1. Beck JL and Katafygiotis LS (1998), Updating models and their uncertainties I: Bayesian statistical framework, Journal of Engineering Mechanics, ASCE, 124(4): 455-461.
2. Beck JL and Yuen KV (2004), Model selection using response measurement: A Bayesian probabilistic approach, Journal of Engineering Mechanics, ASCE, 130(2): 192-203.
3. Chang CC and Chen LW (2003), Vibration damage detection of a Timoshenko beam by spatial wavelet based approach, Applied Acoustics, 64: 1217-1240.
4. Chen WF and Kishi N (1989), Semirigid steel beam-to-column connections: data base and modeling, Journal of Structural Engineering, 116(1): 105-119.

5. Gull SF (1988), Bayesian inductive inference and maximum entropy, maximum entropy and Bayesian methods (Ed. J. Skilling), Kluwer Academic Publisher, Boston: 53-74.

6. Hou Z, Noori M and Amand R (2000), Wavelet-based approach for structural damage detection, J. Eng. Mech. Div. Am. Soc. Civ. Eng., 12(7): 677-683.

7. Katafygiotis LS and Lam HF (2002), Tangential-projection algorithm for manifold representation in unidentifiable model updating problems, Earthquake Engineering & Structural Dynamics, 31 (4): 791-812.

8. Katafygiotis LS, Lam HF and Papadimitriou C (2000), Treatment of unidentifiability in structural model updating, Advances in Structural Engineering, 3(1): 19-39.

9. Katafygiotis LS, Papadimitriou C and Lam HF (1998), A probabilistic approach to structural model updating, Soil Dynamics and Earthquake Engineering, 17(7-8): 495-507.

10. Lam HF and Ng CT (2006), Detection of cracks on a beam by Bayesian model class selection utilizing dynamic data, the 5th International Conference on Computational Stochastic Mechanics (CSM5), June 21-23, 2006, Rhodes, Greece.

11. Lam HF, Lee YY, Sun HY, Cheng GF, and Guo X (2005), Application of the spatial wavelet transform and Bayesian approach to the crack detection of a partially obstructed beam, Thin-Walled Structures, 43: 1-21.

12. Liew KM and Wang Q (1998), Application of wavelet theory for crack identification in structures, Journal of Engineering Mechanics, ASCE, 124: 152-157.

13. Lu CJ and Hsu YT (2002), Vibration analysis of an inhomogeneous string for damage detection by wavelet transform, International Journal of Mechanical Sciences, 44: 745-754.

14. Okafor AC and Dutta A (2000), Structural damage detection beams by wavelet transforms, Smart Mater. Struct. 9: 906-917.

15. Ostachowicz WM and Krawczuk M (1991), Analysis of the effect of cracks on the natural frequencies of a cantilever beam, Journal of Sound and Vibration, 150(2): 191-201.

16. Papadimitriou C, Beck JL and Katafygiotis LS (1997), Asymptotic expansions for reliability and moments of uncertain systems, Journal of Engineering Mechanics, ASCE, 123(12): 1219-1229.

17. Sohn H, Farrar CR, Hernez FM, Czarnecki JJ, Shunk DD, Stinemates DW and Nadler BR (2004), A review of structural health monitoring literature: 1996 – 2001, Los Alamos National Laboratory Report, LA-13976-MS.

18. Spanos PD, Failla G, Santini A and Pappatico M (2006), Damage detection in Euler-Bernoulli beams via spatial wavelet analysis, Structural Control and Health Monitoring, 13: 472-487.

19. Sun Z and Chang CC (2003), Structural Damage Assessment Based on Wavelet Packet Transform, Journal of Structural Engineering, 128(10): 1354-1361.

20. Wang Q and Deng X (1999), Damage detection with spatial wavelets, international Journal of Solids and Structures, 36: 3443-3468.

21. Yan YJ and Yam LH (2002), Online detection of crack damage in composite plates using embedded piezoelectric actuators/sensors and wavelet analysis, Composite Structures, 58: 29-38.

Figure captions

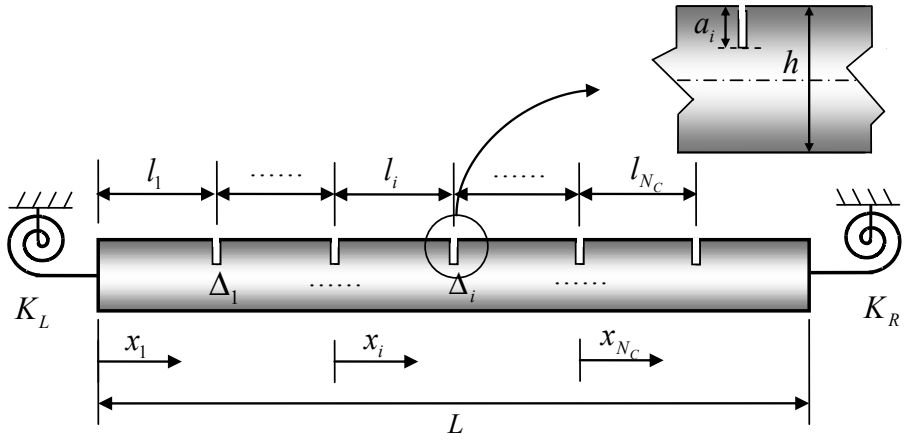

Figure 1: The model of a cracked beam with semi-rigid connections at both ends.

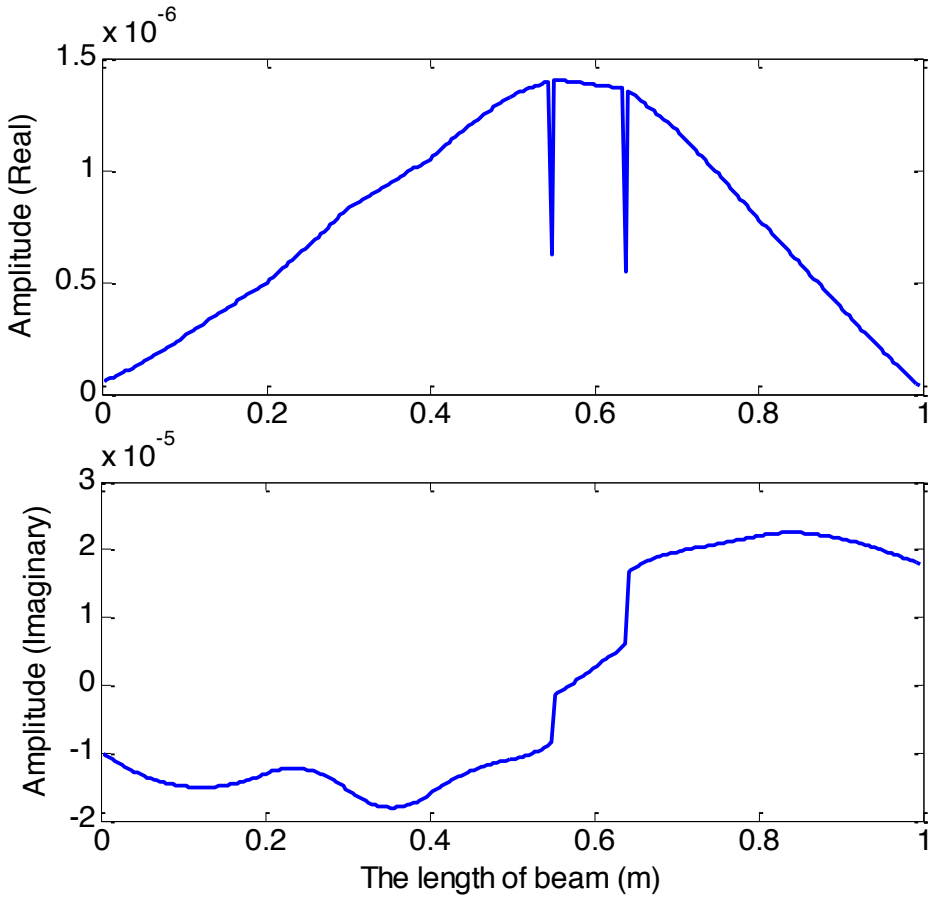

Figure 2: The spatial wavelet transform of the measured response at time $t = 0.07$ sec ($l_1 = 0.55$, $l_2 = 0.09$, $\Delta_1 = 0.1$, $\Delta_2 = 0.15$, $b = 8$).

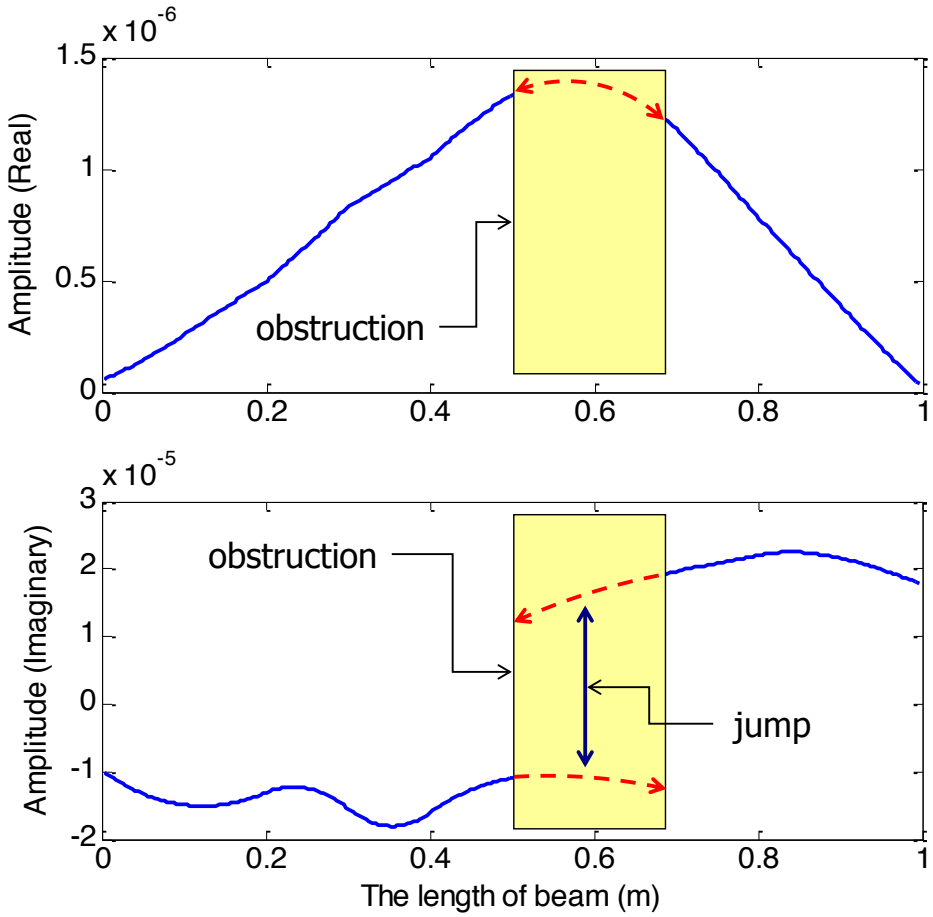

Figure 3: Illustrative diagram showing the possibility of using the imaginary part of the spatial wavelet transform in detecting obstructed cracks.

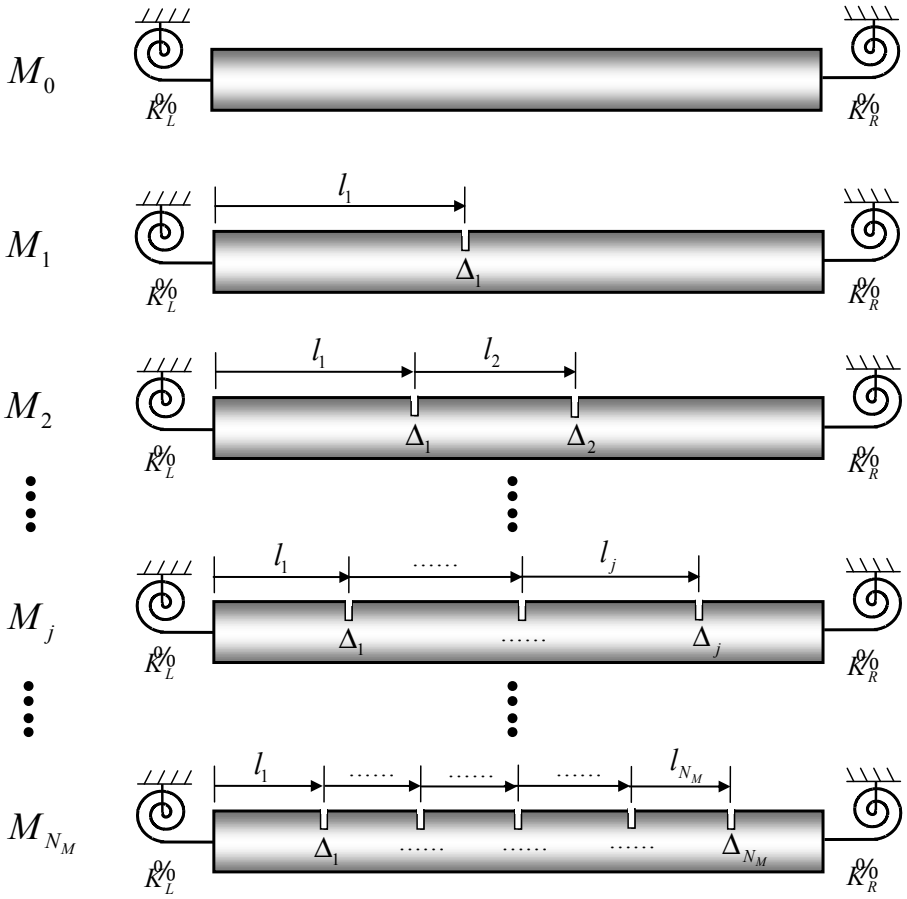

Figure 4: Schematic diagram illustrating the basic strategy for identifying the number of cracks.

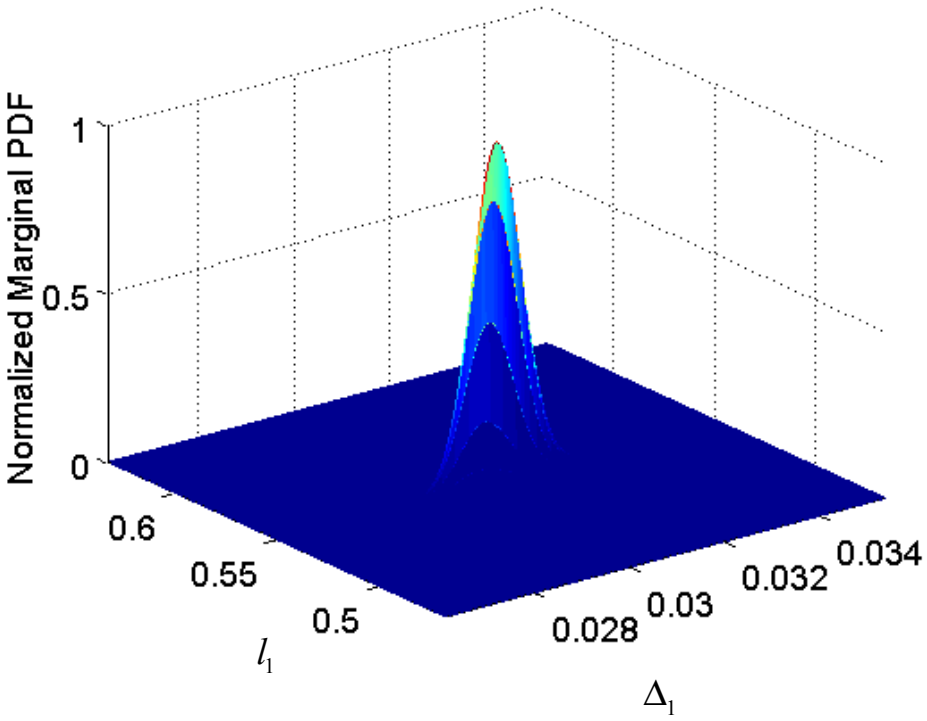

Figure 5: Normalized marginal PDF of the crack location (l_1) and extent (Δ_1) in Case B.

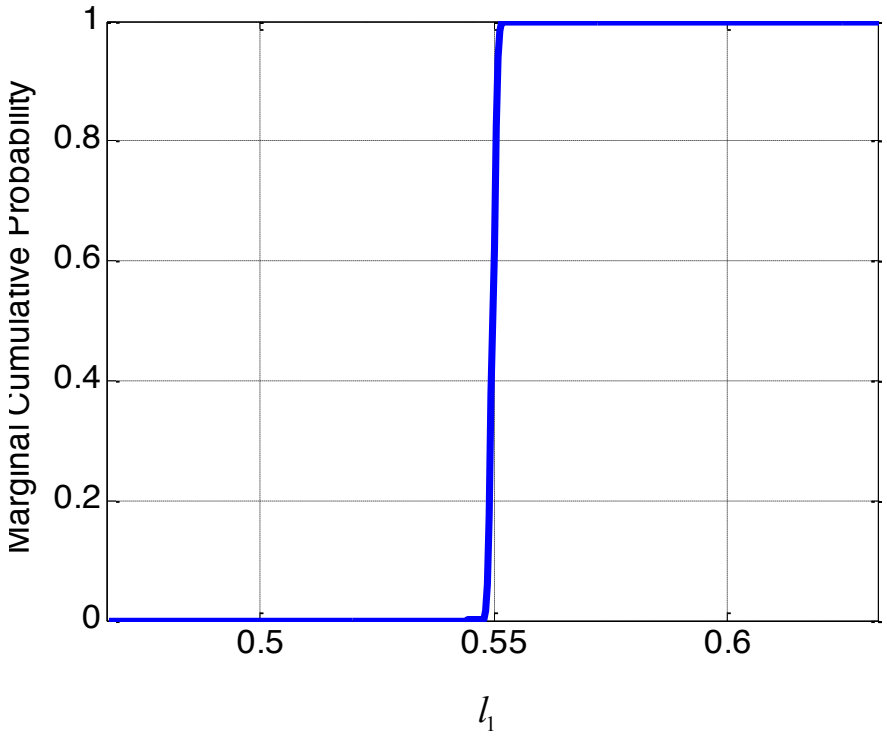

Figure 6: Marginal cumulative distribution of the crack location (l_1) in Case B.

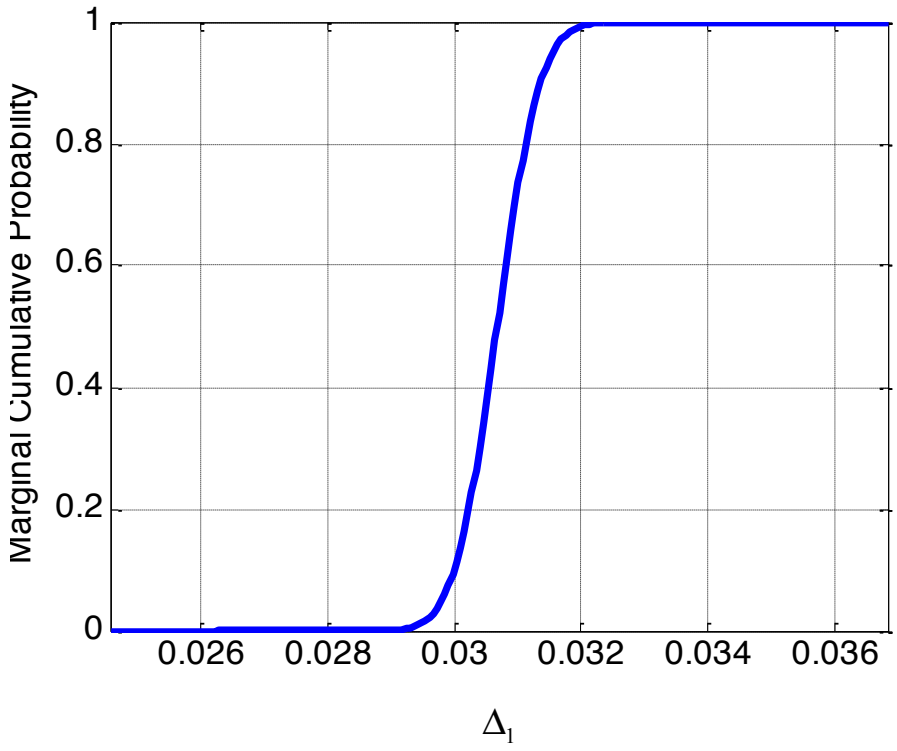

Figure 7: Marginal cumulative distribution of the crack extent (Δ_1) in Case B.

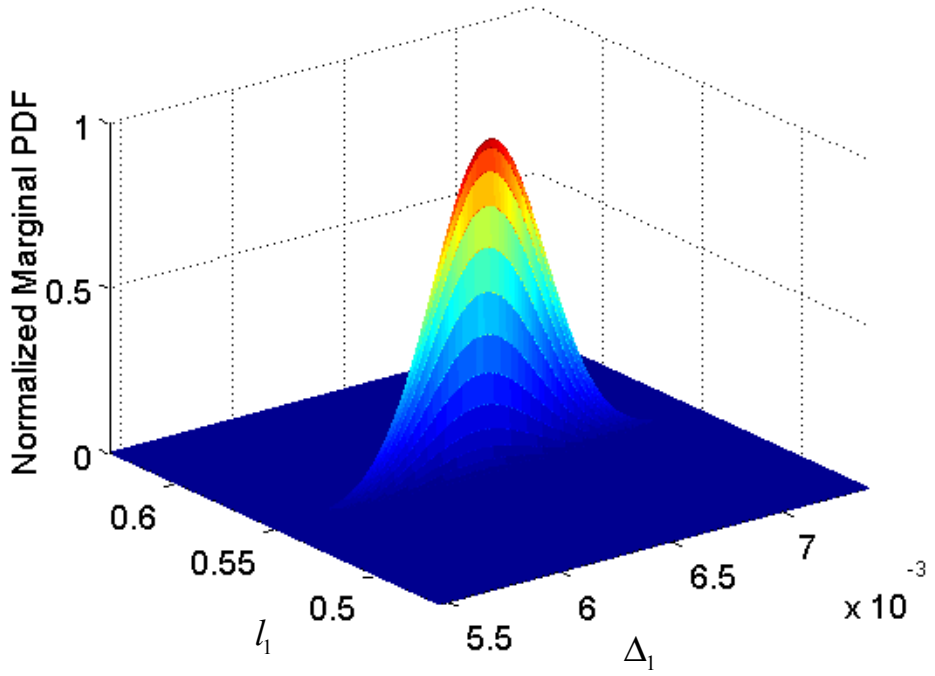

Figure 8: Normalized marginal PDF of the crack location (l_1) and extent (Δ_1) in Case C.

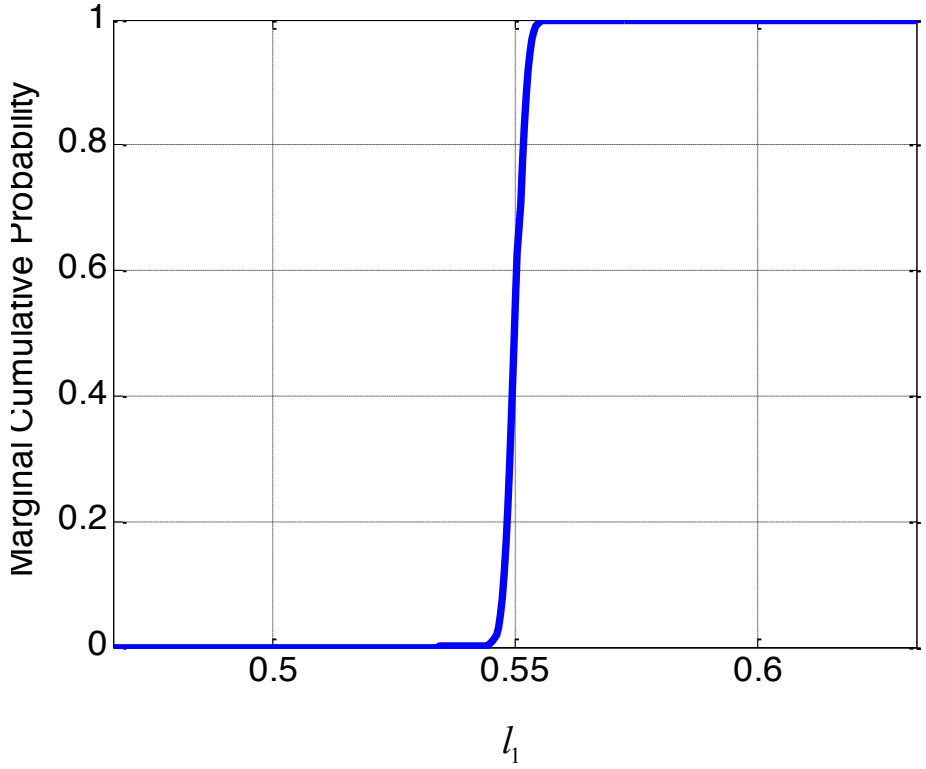

Figure 9: Marginal cumulative distribution of the crack location (l_1) in Case C.

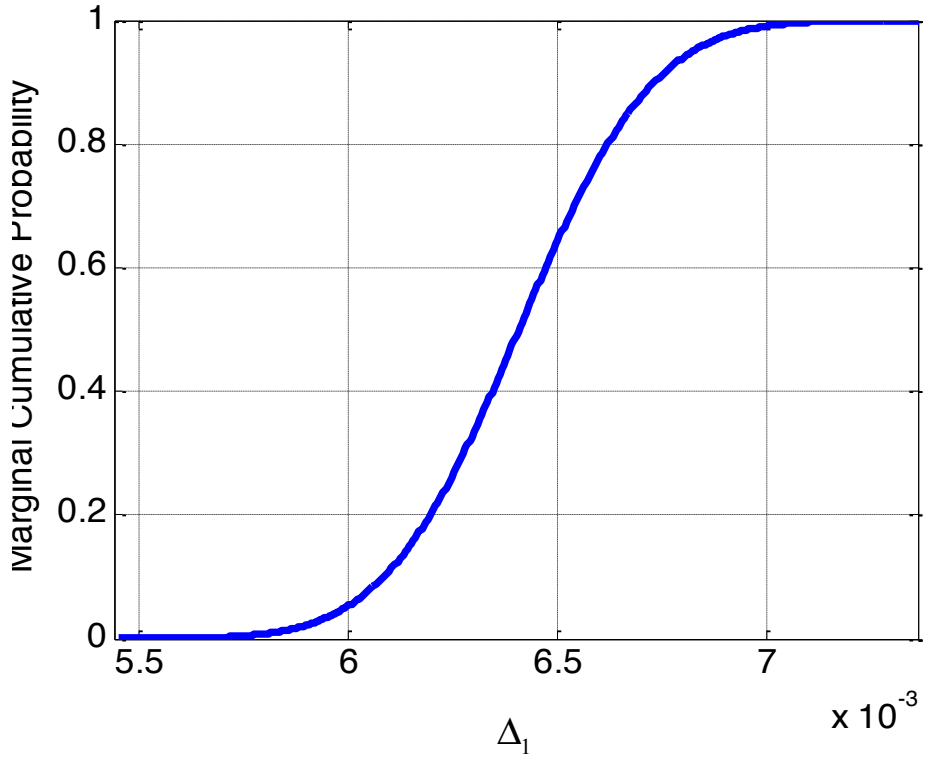

Figure 10: Marginal cumulative distribution of the crack extent (Δ_1) in Case C.

Table captions

Property	Value
Length (L)	1 m
Sectional area (A)	0.0001 m^2
Young's modulus (E)	190 GPa
Mass per unit length (m)	0.7850 kg/m

Table 1: Member properties of the beam used in the numerical case study.

Case	N_C	$(\widetilde{K}_L, \widetilde{K}_R)$	Crack Information
A	0	(0.4, 0.2)	N/A
B	1	(0.4, 0.2)	$l_1 = 0.55,\ \Delta_1 = 0.03$
C	1	(0.4, 0.2)	$l_1 = 0.55,\ \Delta_1 = 0.01$
D	2	(0.4, 0.2)	$l_1 = 0.55,\ \Delta_1 = 0.03$ $l_2 = 0.09,\ \Delta_2 = 0.05$
E	2	(0.4, 0.2)	$l_1 = 0.55,\ \Delta_1 = 0.01$ $l_2 = 0.09,\ \Delta_2 = 0.01$
F	3	(0.4, 0.2)	$l_1 = 0.55,\ \Delta_1 = 0.03$ $l_2 = 0.09,\ \Delta_2 = 0.05$ $l_3 = 0.06,\ \Delta_3 = 0.04$

Table 2: Summary of all cases in the numerical case study.

Case	Class of models	Relative $P(M_j \mid D,U)$	Logarithm of the		
			Evidence	Likelihood factor	Ockham factor
A	M_0	**1.0**	45101	45120	-19
	M_1	6.6×10^{-5}	45091	45121	-30
B	M_0	2.9×10^{-640}	43517	43535	-18
	M_1	**1.0**	44990	45022	-32
	M_2	1.2×10^{-4}	44981	45023	-42
C	M_0	3.0×10^{-105}	44915	44933	-18
	M_1	**1.0**	45155	45187	-32
	M_2	1.1×10^{-3}	45149	45188	-39
D	M_0	5.5×10^{-1891}	40599	40615	-16
	M_1	6.4×10^{-170}	44562	44594	-32
	M_2	**1.0**	44951	44996	-45
	M_3	1.6×10^{-3}	44945	45001	-56
E	M_0	4.0×10^{-277}	44530	44549	-19
	M_1	4.4×10^{-55}	45042	45073	-31
	M_2	**1.0**	45167	45211	-44
	M_3	3.5×10^{-4}	45159	45218	-59
F	M_0	1.7×10^{-3364}	37166	37180	-14
	M_1	1.5×10^{-688}	43328	43358	-30
	M_2	2.5×10^{-61}	44772	44818	-46
	M_3	**1.0**	44911	44969	-58
	M_4	5.8×10^{-3}	44906	44972	-66

Table 3: Model class selection results for all cases

Case	Crack location l_j (COV %)	Crack extent Δ_j (COV %)
A	N/A	N/A
B	l_1: 0.5499 (0.12)	Δ_1: 0.0307 (1.74)
C	l_1: 0.5502 (0.34)	Δ_1: 0.0064 (3.93)
D	l_1: 0.5403 (0.21) l_2: 0.0945 (0.08)	Δ_1: 0.0260 (2.23) Δ_2: 0.0537 (0.80)
E	l_1: 0.5592 (0.45) l_2: 0.0890 (0.27)	Δ_1: 0.0069 (4.58) Δ_2: 0.0083 (4.17)
F	l_1: 0.5513 (0.18) l_2: 0.0873 (0.32) l_3: 0.0586 (0.33)	Δ_1: 0.0326 (1.87) Δ_2: 0.0465 (4.74) Δ_3: 0.0436 (6.22)

Table 4: Identified crack locations, extents and corresponding COV in all cases

Normalized spring stiffness (COV %)		Damping Ratio ζ (COV %)
$K_L^{\%}$	$K_R^{\%}$	
0.4021 (3.72)	0.1981 (7.06)	0.0098 (0.47)
0.4105 (3.79)	0.1971 (7.79)	0.0101 (0.47)
0.4105 (3.79)	0.1498 (9.77)	0.0099 (0.47)
0.3789 (3.95)	0.2178 (6.16)	0.0101 (0.47)
0.4196 (3.70)	0.1363 (10.22)	0.0099 (0.46)
0.4106 (3.83)	0.2103 (6.10)	0.0100 (0.47)

Table 5: Identified model parameters and corresponding COV in all cases